*Sciences & Technologie A* – **N°42, Décembre 2015**, 41-48.

# TRANSIENT LAMINAR SEPARATED FLOW AROUND AN IMPULSIVELY STARTED SPHERICAL PARTICLE AT 20≤RE≤1000

**BENABBAS FARIDA AND BRAHIMI MALEK**
University A. MIRA of Bejaïa, Faculty of Technology, Department of Process Engineering,
Targa-Ouzemour,Bejaia,Algeria

*Reçu le 02/08/2013 – Accepté le 24/06/2015*

**Résumé**

Les simulations numériques des caractéristiques de l'écoulement laminaire axisymétrique autour d'une sphère rigide en démarrage impulsif, sont présentées pour des nombres de Reynolds variant entre 20 et 1000. Les résultats sont obtenus par résolution de l'équation de Navier-Stokes complète, instationnaire dans sa formulation rotationnel-fonction de courant. Un schéma numérique compact précis à l'ordre 4 est utilisé pour la discrétisation de l'équation de Poisson pour la fonction de courant et est combiné à la méthode implicite aux directions alternées pour l'équation de transport de la vorticité. Nous présentons l'évolution temporelle de l'angle de séparation et de la longueur du tourbillon. Nous examinons aussi la variation au cours du temps de la vitesse axiale et de la vorticité autour de la sphère. Le tourbillon secondaire est initié au temps adimensionné 5 pour un Reynolds proche de 610. Les données numériques et expérimentales, dans le cas stationnaire, disponibles dans la littérature présentent une bonne concordance avec nos résultats.

**Mots clés :**Ecoulement transitoire, hermitian compact, longueur de vortex, ,sphère

**Abstract**

Numerical simulations of the axisymmetric laminar flow characteristics past a rigid sphere impulsively started are presented for Reynolds numbers from 20 to 1000. The results are obtained by solving the complete time dependant Navier-Stokes equations in vorticity and stream function formulation. A fourth order compact method is used to discretize the Poisson equation of stream function while the vorticity transport equation is solved by an alternating direction implicit method. Time evolution of flow separation angle and length of the vortex behind the sphere are reported. Time variation of the axial velocity in the vortex and the wall vorticity around the sphere are also examined. Secondary vortices are seen to be initiated at Reynolds number of 610 and for dimensionless time t about 5. Comparisons with previously published simulations and experimental data for steady state conditions show very good agreement.

***Keywords:*** transient flow, hermitian compact, vortex length, drag, sphere

**ملخص.**

**محاكاة عددية لخصائص الانسياب الطبقي المتماثل محوريا حول جسم كروي صلب دو الحركة الدافعة مقدمة لأعداد رينولدس بين 20 و 1000 .تحصلنا على النتائج بتحليل معادلة نافيي ستوكس الكاملة و المحظرة على شكل دالة التيار والدوران الدوامي.**
**طريقة التفصيل العددي المستعملة لتحليل معادلة بواسون بدقة من الدرجة الرابعة هي طريقة متضامه استعملت بسياق طريقة "الاديئي" .**
**نقدم نتائج التطور الزمني لزاوية الانفصال السيلان من الجسم الكروي و طول الحركة الدوامية. قدمنا كذالك التطور مع الزمن للسرعة المحورية داخل الدوامة و قيمة الدوامة على سطح الجسم الكروي. بينت المحاكاة العددية ميلاد الدوامة الثانوية قرابة عدد رينولدس 610 في الزمن 5 .**
**المقارنات مع المحاكاة المنشورة سابقا والبيانات التجريبية تبين أتفاقا جيد بالنسبة للسيلان المستقر.**

***الكلمات المفتاحية:*** تدفق عابرة، الهرميتي المدمجة، طول دوامة، المجال

## Introduction :

The steady and unsteady viscous flows over a spherical particle have been extensively studied by different numerical approaches and experimental methods (Rimon and Cheng (1969),Benabbas (1987) Fornberg (1988), Johnson and Patel (1999), Lee (2000), Benabbas et al. (2003), Gushchin and Matyushin (2006), Sekhar et al. (2012)). The transient development of the momentum transfer or heat and mass transfer around a sphere has received rather much less attention (Benabbas and Brahimi (2012)). The accelerating conditions of the particle motion have been considered in numerical studies at moderate Reynolds numbers (Lin and Lee (1973), Reddy et al. (2010)). In the present paper, the time evolution of the flow induced by an impulsively started sphere is considered for Reynolds numbers up to 1000. This case constitutes a reference model for more complex practical situations such as the behaviour of the flow around particles in fluidizing systems (Kechroud et al. (2010a,b)). Similar problem for the cylinder has been investigated numerically (Ta Phuoc Loc and Bouard (1985), Thoman and Szewczyk (1969), Collins and Dennis (1973) and experimentally (Bouard and Coutanceau (1980)). A very good agreement between the simulations and the experimental results was observed including the complex structure of the secondary vortices. We have used the same efficient numerical method to conduct the analysis of the separated laminar flow over a sphere. The numerical method is based on a high-order compact scheme for spatial discretization of the stream function equation and a second-order one (ADI) to handle the vorticity equation while the time discretization is of second-order accuracy. The transient development of the flow is examined through the presentation of its main characteristics. Time evolution of the separation angle with Reynolds number is presented. The wall vorticity behavior for increasing time and Reynolds number is analyzed. The length of the recirculation region with time behind the sphere is also reported. The magnitude of axial velocities in the vortex illustrates the increasing strength of flow mixing with time and Reynolds number. The Steady state results of drag coefficient, angle of separation and length of the recirculation region compare very well with those obtained by different numerical methods in previous works.

## 2-Mathematical formulation

### 2.1 governing equations

The governing equations for the present purpose are the equations of conservation of mass (continuity) and momentum (Navier-Stokes ), they are written in vector form with dimensionless variables as:

$$div\vec{V} = 0 \qquad (1)$$

$$\frac{Re}{2}\left(\frac{\partial \vec{V}}{\partial t} + \overrightarrow{rot}\ \vec{V}X\vec{V} + \overrightarrow{grad}\ \frac{V^2}{2}\right) = \Delta\vec{V} - \overrightarrow{grad}\ \hat{p} \qquad (2)$$

In this simulation the velocity vector $\vec{V}$ has two components $V_r(r,\theta)\ and\ V_\theta(r,\theta)$, $\hat{p} = p + \rho g z$ where p is the static pressure and $\rho$ the fluid density , g the gravitational acceleration ad z is the height . $Re = 2aV_\infty/\nu$ , is the Reynolds number based on the sphere diameter 2a, twice the radius a; the velocity of the fluid far from the sphere $V_\infty$ and ν is the kinematic viscosity .We used in equations (1) and (2) the dimensionless variables defined as : $r = r^*/a$ ; $V_r = V_r^*/V_\infty$ ; $V_\theta = V_\theta^*/V_\infty$ ; $t = t^*V_\infty/a$ ; $\hat{p} = \hat{p}^*/\rho V_\infty^2$ ; the asterisk indicates the dimensional variables.

Equations (1) and (2) are applied on the domain $1 \le r \le (r_\infty/a) and\ 0 \le \theta \le \pi$ accompanied with the boundary conditions which are: the no slip condition on the surface of the sphere , $r = 1, V_r = V_\theta = 0$ and the uniformity of the flow far from the obstacle, $r = {}^{r_\infty}/_{a}$ , $V_r = cos\theta\ and\ V_\theta = -sin\theta$ .

In addition we get the axisymetric hypothesis of the flow around the sphere.

First of all the unsteady Navier-Stokes equations are rewritten in vorticity and stream function formulation. We have used, for this purpose, the coordinate transformation $\xi = \ln(r)$ to refine the mesh in the vicinity of the sphere, where gradients may be important, without increasing the number of nodes, otherwise in the angular direction we change only the name of the variable $\eta = \theta$, the transformed domain is then $\xi \in \{1, \xi_\infty\}\ and\ \ \eta \in \{0, \pi\}$.

The numerical methodology begins with the first equation (1), it's used to define the stream function we have:

$$V_\xi = \frac{e^{-2\xi}}{\sin\eta}\frac{\partial\psi}{\partial\eta}\ \ ;\ \ V_\eta = -\frac{e^{-\xi}}{\sin\eta}\frac{\partial\psi}{\partial\xi} \qquad (3)$$

Equation (2) is transformed from it's original form when we take it's rotational, the term of pression get out and we have:

$$e^{\xi}\frac{\partial\omega}{\partial t} + V_\xi\frac{\partial\omega}{\partial\xi} + V_\eta\frac{\partial\omega}{\partial\theta} - \left(V_\xi + V_\eta\cot\eta\right)\omega = \frac{2}{\mathrm{Re}}e^{-\xi}\left(D^2\omega - \frac{\omega}{\sin^2\eta}\right)$$

$D^2$ is a differential operator

$$D^2 = \frac{\partial^2}{\partial\xi^2} + \frac{\partial}{\partial\xi} + \cot\eta\frac{\partial}{\partial\eta} + \frac{\partial^2}{\partial\eta^2} \qquad (4)$$

Otherwise the definition $\vec{\omega} = \overrightarrow{rot}\vec{V}$ is developped in spherical coordinates then the velocity components are replaced with the first derivatives of the stream function defined from the continuity equation

$$e^{3\xi} sin\eta.\omega = \frac{\partial\psi}{\partial\xi} - \frac{\partial^2\psi}{\partial\xi^2} + cot\eta.\frac{\partial\psi}{\partial\eta} - \frac{\partial^2\psi}{\partial\eta^2} \qquad (4)$$

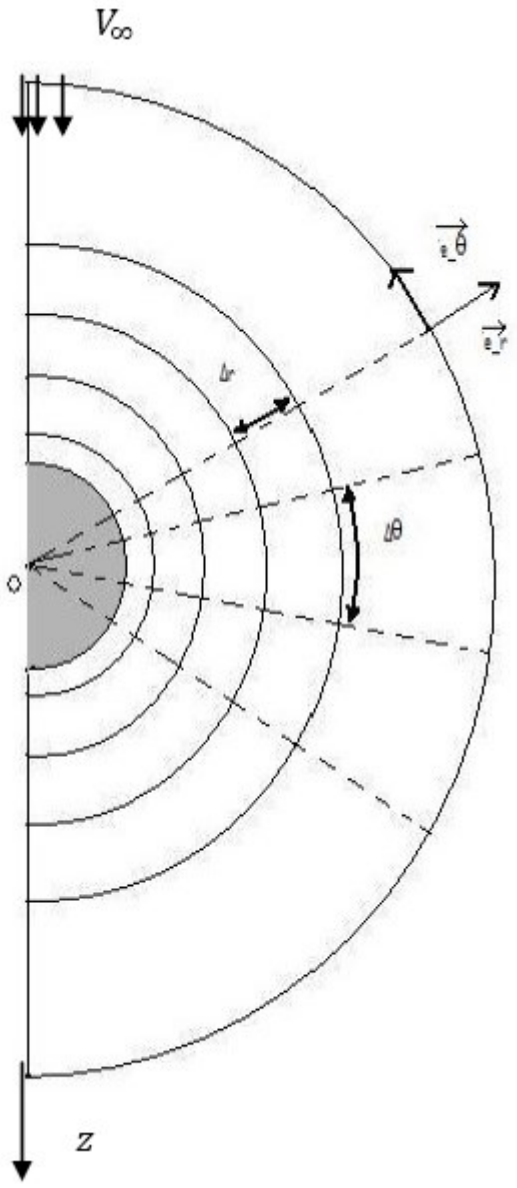


Figure 1 schematic spatial domain

Each point of the transformed domain $[0 \le \xi \le \xi_\infty\ ,\ 0 \le \eta \le \pi]$ is specified by it's indices:

$\xi_i = (i-1)\Delta\xi$ and $\eta_j = (j-1)\Delta\eta$ with $i = 1, \dots, NI$ and $j = 1, \dots, NJ$

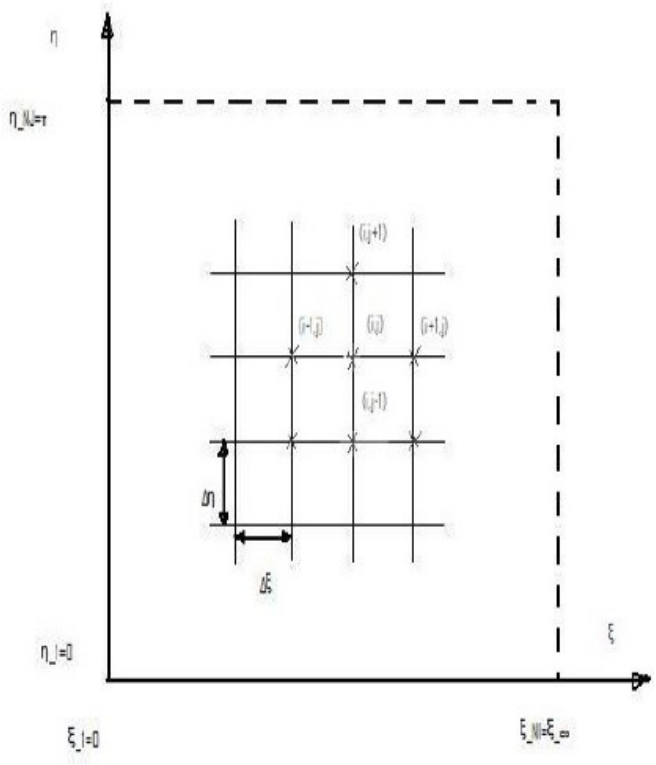


Figure 2 transformed domain mesh

## 2.2 Initial and boundary conditions

Since the simulation is concerned with an impulsively started movement, all dependant variables are equal to zero at initial time $t = 0$.

Otherwise the boundary conditions of the problem are translated in terms of the variables $\omega$; $\psi$ and the derivatives of . Therefore, we can write on the sphere $(\xi = 0)$

$$\psi(0,\eta) = 0 \quad and \quad \frac{\partial\psi}{\partial\xi}(0,\eta) = \frac{\partial\psi}{\partial\eta}(0,\eta) = 0$$

$$\frac{\partial^2\psi}{\partial\xi^2}(0,\theta) = -\sin\eta.\omega(0,\eta) \quad \text{from equation (4)}$$

for surface conditions on the vorticity, we have drawn a relation from the fourth order Taylor expansion of the stream function $\psi$ using only the first two nodes in the radial direction $\xi$; after that derivatives of $\psi$ are replaced and then we obtain:

$$\omega(0,\theta).(2+4\Delta\xi) + \omega(\Delta\xi,\eta) = \frac{-6}{\sin\eta.\Delta\xi^2}.(\psi(\Delta\xi,\eta) - \psi(0,\eta)) \qquad (5)$$

The conditions far from the sphere are those of an irrotational flow, so they are expressed for t ≥ 0 as:
$\omega(\xi_\infty,\eta) = 0$ and $\psi(\xi_\infty,\eta) = \frac{1}{2}e^{2\xi_\infty}sin^2\eta$

The first and second partial derivatives of $\psi(\xi,\eta)$ can be easily derived from $0.5e^{2\xi}sin^2\eta$.
The axisymetric hypotheses enforce the conditions

$\omega(\xi,0) = 0 = \omega(\xi,\pi)$
$\psi(\xi,0) = 0 = \psi(\xi,\pi)$
$\psi\eta\eta$ *is an even function*

### 3-Methodology of resolution

The numerical method used in our simulation is presented for the first time in Bontoux (1978) and has proven its efficiency to simulate the flow over an impulsively started cylinder (Ta Phuoc Loc (1980), Ta Phuoc Loc and Bouard (1985). We have extended the use of this method for the study of the viscous flow over a sphere at moderate and high Reynolds numbers (Benabbas (1987)).
Because of the absence of boundary conditions on the rotational derivatives, the transport of rotational equation is not treated by the compact scheme. And it's the stream function equation witch benefits from enough conditions on all derivatives . So the use of Hermitian compact for equation (8) accompanied with the closure relations from the Merhstellen method [Cf. benabbas], for the derivatives $\psi\xi,\ \psi\xi\xi,\ \psi\eta\eta$ *and* $\psi\eta\eta$:
Equation (8) is rewritten in an pseudo unsteady form and we use Optimum convergence coefficients $\lambda_{kh}$ *et* $\lambda_{kv}$ of WASCHPRESS [ cf. benabbas] they are calculated for $2^N$ iterations.

$$\frac{\partial\psi}{\partial\tau}_{i,j} + \psi\xi_{i,j} - \psi\xi\xi_{i,j} + cot\eta_j\psi\eta_{i,j} - \psi\eta\eta_{i,j} = e^{3\xi_i}sin\eta_j\omega_{i,j} \qquad (6)$$

For each iteration, equation (9) is discretised relative to only one direction so
in radial direction we have:

$$\lambda_{kh}\psi_{ij}^{p+\frac{1}{2}} + \psi\xi_{ij}^{p+\frac{1}{2}} - \psi\xi\xi_{ij}^{p+\frac{1}{2}} = (\lambda_{kh}\psi - cot\eta\psi\eta + \psi\eta\eta)_{ij}^{p} + e^{3\xi_i}sin\eta_j\omega_{ij}^{n} \qquad (7)$$

$$\frac{3}{\Delta\xi}(\psi_{i+1,j} - \psi_{i-1,j}) - (\psi\xi_{i+1,j} + 4\psi\xi_{i,j} + \psi\xi_{i-1,j}) = 0$$

$$\frac{12}{\Delta\xi^2}(\psi_{i+1,j} - 2\psi_{i,j} + \psi_{i-1,j}) - (\psi\xi\xi_{i+1,j} + 10\psi\xi\xi_{i,j} + \psi\xi\xi_{i-1,j}) = 0$$

With the boundary conditions
$\psi_{1,j} = \psi\xi_{1,j} = 0$
$\psi\xi\xi_{1,j} = -\sin\eta_j \quad \omega_{1,j}$

$$\psi_{NI,j} = \frac{1}{2}e^{2\xi_{NI}}sin^2\eta_j$$

$$\psi\xi_{NI,j} = 2\psi_{NI,j} \ ; \ \psi\xi\xi_{NI,j} = 4\psi_{NI,j}$$

And in angular direction we have

$$\lambda_{kv}\psi_{ij}^{p+1} + cot\eta_j\psi\eta_{ij}^{p+1} - \psi\eta\eta_{ij}^{p+1} = (\lambda_{kv}\psi - \psi\xi + \psi\xi\xi)_{ij}^{p+1/2} - e^{3\xi_i}sin\eta_j\omega_{ij}^{n}$$

$$\frac{3}{\Delta\eta}(\psi_{i,j+1} - \psi_{i,j-1}) - (\psi\eta_{i,j+1} + 4\psi\eta_{i,j} + \psi\eta_{i,j-1}) = 0$$

$$\frac{12}{\Delta\eta^2}(\psi_{i,j+1} - 2\psi_{i,j} + \psi_{i,j-1}) - (\psi\eta\eta_{i,j+1} + 10\psi\eta\eta_{i,j} + \psi\eta\eta_{i,j-1}) = 0$$

With bounady conditions :
$\psi_{i,1} = \psi\eta_{i,1} = 0$
$\psi\eta\eta_{i,1}$ *est une fonction paire*
$\psi_{i,NJ} = \psi\eta_{i,NJ} = 0$
$\psi\eta\eta_{i,NJ}$ *est une fonction paire*
Regarding to the transport equation, The Peaceman – Rachford A.D.I. scheme is applied to the vorticity transport equation (6). The temporal evolution from $t\ to\ t+\Delta t$ is calculated in two steps, first of all $from\ t\ to\ t+\frac{\Delta t}{2}$ $then\ from\ t+\frac{\Delta t}{2}\ to\ t+\Delta t$, we have
First step of the resolution:
In the angular direction $\eta$ equation (6) :

$$e^{\xi}\left(\frac{\partial\omega}{\partial t}\right)^{n+\frac{1}{2}} + V_\eta^n(\omega\eta)^{n+\frac{1}{2}} - (V_\xi + V_\eta\cot\eta)^n\omega^* - \frac{2}{Re}e^{-\xi}\left(\cot\eta\,\omega^{n+\frac{1}{2}} + \omega\eta\eta^{n+\frac{1}{2}}\right) = \frac{2}{Re}e^{-\xi}\left(\omega\xi\xi^n + \omega\xi^n - \frac{\omega^n}{sin^2\eta}\right) - V_\xi^n \quad \omega\xi^n$$

$\omega^*$ will correspond to either $\omega^{n+1}$ or $\omega^{n+1/2}$ depending on whether the term $(V_\xi + V_\eta\cot\eta)$ has positive or negative value, in order to reinforce the principal diagonal.

Resulting in the tridiagonal equations :

$$A_1\omega_{i,j-1}^{n+1/2} + B_1\omega_{i,j}^{n+1/2} + C_1\omega_{i,j+1}^{n+1/2} = D_1$$
$for\ j = 2,\dots,NJ-1$
With the conditions $\omega_1 = \omega_{NJ} = 0$
And in the second time step:

$$e^{\xi}\left(\frac{\partial\omega}{\partial t}\right)^{n+1} + V_\xi^n(\omega\xi)^{n+1} - (V_\xi + V_\eta\cot\eta)^n\omega^* - \frac{2}{Re}e^{-\xi}(\omega\xi\xi + \omega\xi)^{n+1} = \frac{2}{Re}e^{-\xi}\left(cot\eta.\,\omega\eta^{n+1/2} + \omega\eta\eta^{n+1/2} - \frac{\omega^n}{sin^2\eta}\right) - V_\eta^n \quad \omega\eta^{n+1/2}$$

Then we develop $\omega\xi$ *and* $\omega\xi\xi$ and then gather identical multiplier terms to get

$$A_2\omega_{i-1,j}^{n+1} + B_2\omega_{i,j}^{n+1} + C_2\omega_{i+1,j}^{n+1} = D_2$$
$for\ i = 2,\dots,NI-1$
Completed With the discretisation of parietal condition on the rotational (10)

$$\omega_{1,j}(2+4\Delta\xi) + \omega_{2,j} = \frac{-6}{sin\eta_j\Delta\xi^2}(\psi_{2,j} - \psi_{1,j})$$

And the irrotational flow far from the sphere :

$\omega_{NI,1} = 0$

The method combines two numerical schemes. The classical ADI scheme is used to resolve the transport equation of the vorticity and the other, based on a compact hermitian method, is applied to the Poisson equation of the stream function (Benabbas (1987) for the details). This equation is treated as a parabolic one with the introduction of a pseudo-time and optimum coefficients of convergence are used in the iterative calculations.

In each direction (ξ and η) new dependant variables are taken into account :

$\psi, \frac{\partial \psi}{\partial \xi} and \frac{\partial^2 \psi}{\partial \xi^2}$ for the first half time step and

$\psi, \frac{\partial \psi}{\partial \eta} and \frac{\partial^2 \psi}{\partial \eta^2}$ for the second half time step.

The steady state is determined with a test on the vorticity field $\left|\omega^{n+1} - \omega^{n}\right| \leq \varepsilon = 10^{-4}$.

## 3-Results and discussion

### 3.1 steady state flow characteristics

Time evolution of the laminar separated flow past an impulsively started sphere has been calculated for various Reynolds numbers in the range of 20 to 1000. Before presenting transient dynamic behavior of the flow field, we would like to illustrate the efficiency of the numerical method used by presenting comparisons of our calculations for some important steady state characteristics with published experimental data and simulation results based on different numerical methods.

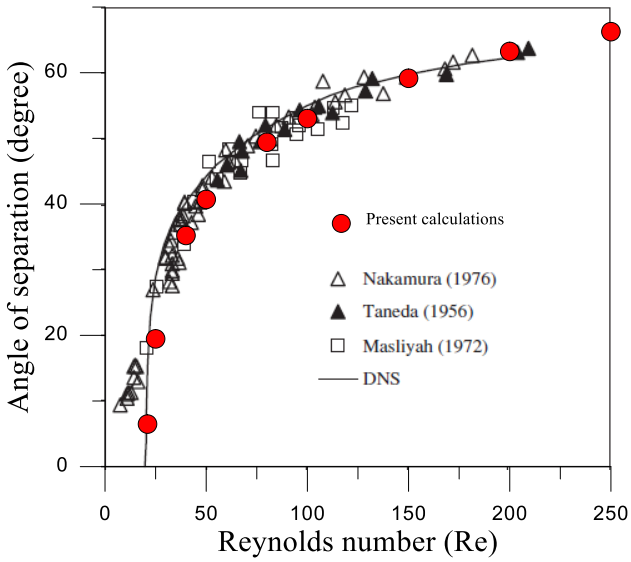


Fig.3: steady state angle of separation

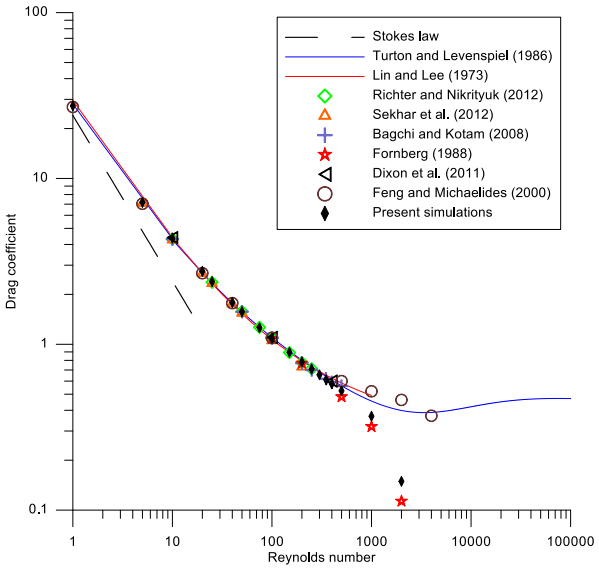


Fig.4: steady state drag coefficient

Figure 3 compares results of the angle of separation and shows very good agreement between practically all the data for the Reynolds numbers considered. The drag coefficient is presented in figure 4 and indicates an excellent agreement with experimental correlations and numerical results of different authors up to Reynolds number of 500. But for higher Reynolds numbers our calculations are close to those of Fornberg (1988) than the simulations of Feng and Michaelides (2001). The vortex length is reported in figure 5 and compared with experimental and numerical data. We observe a satisfactory agreement between them. The DNS results on figures 3 and 5 are of Reddy et al. (2010).

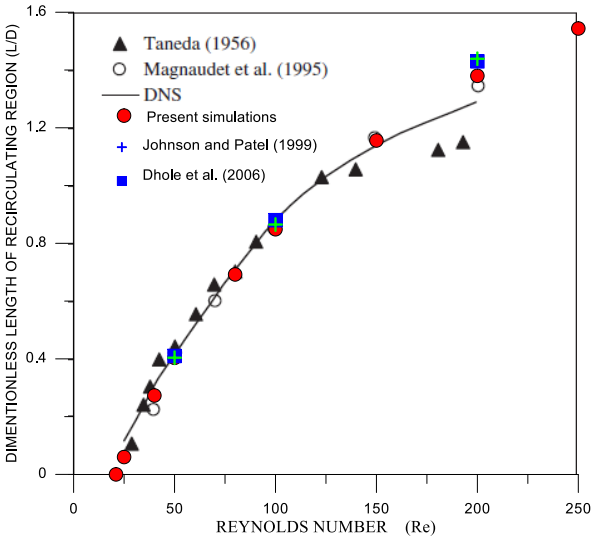


Fig.5: steady state length of recirculation region

All the above confrontations comfort the efficiency and accuracy of the numerical method used in the present study.

### 3.2 transient flow characteristics

Figures 6 and 7 show the vorticity at the surface of the sphere with time for Reynolds number respectively equal to 300 and 1000. The early stages of the flow are characterized by a fast growth of the recirculation region before reaching a slow development towards the steady state.

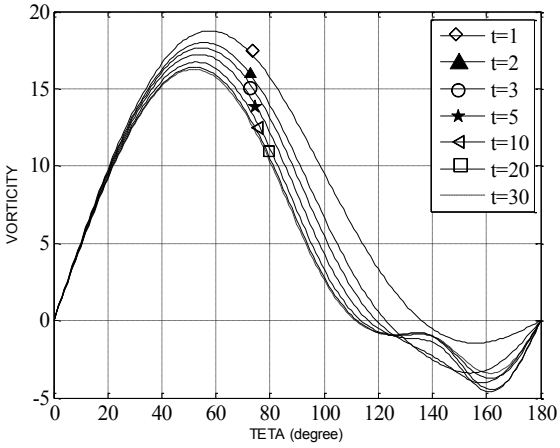


Fig.6: vorticity on the sphere at Re=300

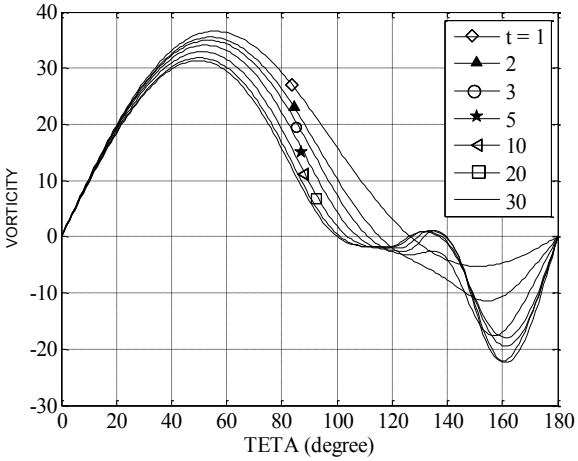


Fig.7: vorticity on the sphere at Re=1000

The sign change of the vorticity observed for Reynolds number of 1000 and time about t=5 indicates the birth of a secondary vortex of weak strength which has opposite rotation to the main vortex. This happens when the back flow itself separates from the sphere. The Reynolds number for which this phenomenon appears first is found to be 610.
In the case of a cylinder and for Reynolds number of 1000 two secondary vortices are observed (Ta Phuoc Loc (1980), Bouard and Coutanceau (1980)).

Figure 8 shows forward separation angle versus time for increasing Reynolds number. At early times the separation point moves at a rapid rate but then slowly approaches its steady state value. The transient length of the vortex behind the sphere for the same Reynolds numbers is reported on figure 7.

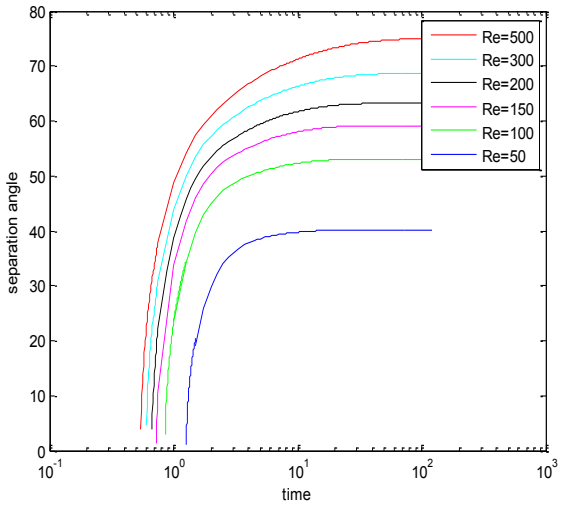


Fig.8: time evolution of separation angle

At the early stages the vortex grows rapidly in size and then followed by a slow approach to its final steady state value. The calculated steady state vortex lengths compare very well with values reported in other numerical and experimental studies as shown above (fig.5).

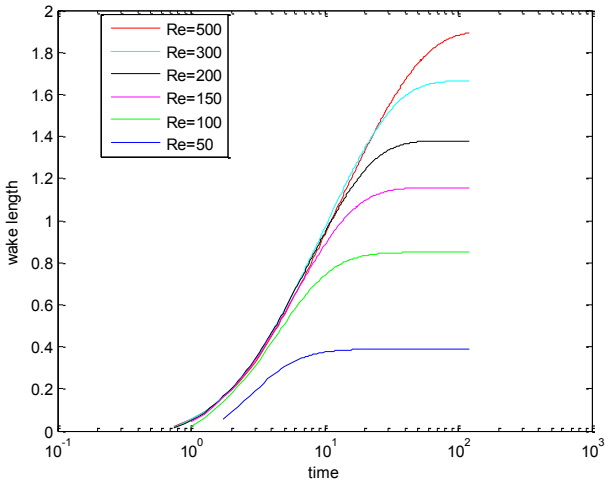


Fig.9: time evolution of vortex length

Figures 10 and 11 illustrate time evolution of the axial velocity on the axis of symmetry behind the sphere for Reynolds numbers of 300 and 1000. We can observe the increasing of the velocity modulus in the vortex region with time and Reynolds number but is limited to values lower than one. In the case of a cylinder, values higher than one are calculated (Ta Phuoc Loc (1980)). The growth of the velocity modulus with time illustrates the action of the convective mixing in the vortex. This action becomes stronger with increasing Reynolds number.

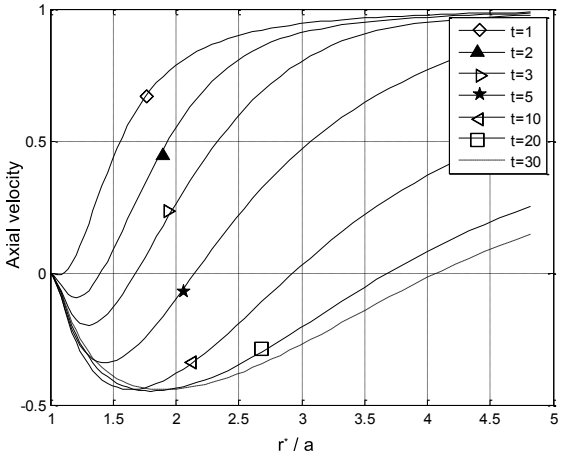


Fig.10: time variation of axial velocity at Re=300

The null value of the velocity on the axis indicates the limit of the vortex region and so its length. For the same time, the vortex length is slightly higher for Re=300 than for Re=1000.

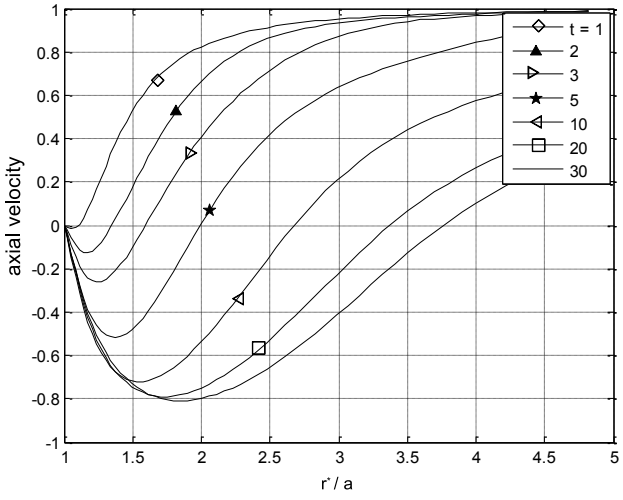


Fig.11: time variation of axial velocity at Re=1000

## CONCLUSION

The complex problem of the transient laminar separated flow over an impulsively started sphere has been conducted with efficient mixed hermitian compact method. The steady state results have been successfully compared to the highest accurate methods used till now. The transient characteristics of the flow have concerned the vorticity on the sphere under the influence of Reynolds number and the results revealed the appearance of secondary vortex at Reynolds number of 610. Time evolution of the separation angle and the vortex length are also presented and the simulations have shown a rapid growth of these characteristics at the early stages of the flow development. The transient behavior of axial velocity behind the sphere indicated how the convective mixing in the vortex increases with time and Reynolds number. The present results constitute a valuable basis to understand the enhancement of heat and mass transfer in cyclic regime of fluidized or fixed beds.

## REFERENCES

1. Bagchi P., Kottam K., 2008. Effect of free stream isotropic turbulence on heat transfer from sphere. Phys. Fluids. 20, 073305.
2. Bontoux P., 1978. Contribution à l'étude des écoulements visqueux en milieu confiné. Analyse et Optimisation de méthodes numériques de haute précision. Thèse de Doctorat ès-sciences, Université d'Aix-Marseille II, France.
3. Benabbas F. ,1987. Etude numérique de l'écoulement autour d'une sphère aux grands nombres de Reynolds en régime stationnaire et instationnaire. Thèse de Doctorat de Troisième cycle. Université de Poitier, France.
4. Benabbas F., Brahimi M., Tighzert H. , 2003. Caractérisation du très proche sillage d'une sphere à des nombres de Reynolds modérés et spectres singuliers . "16ième Congrès Français de Mécanique." , Nice, France, Sep. 1–5, pp. 1–7.
5. Benabbas F., Brahimi M., 2012. Transient mass transfer around an impulsively started spherical particle at low to high Peclet numbers. "The 9th EuroMech Fluid Mech. Conf.", Rome, Italy, Sep. 9-13, accepted.
6. Bouard R., Coutanceau M., 1980. The early stage of development of the wake behind an impulsively started cylinder for $40 \leq Re \leq 10^4$. J. Fluid Mech. 101, 583-607

7. Collins W. M., Dennis S .C. R., 1973. Flow past an impulsively started circular cylinder. J. Fluid. Mech., 60,105-127.

8. Dhole S. D., Chhabra R. P., Eswaran V., 2006. A numerical study on the forced convection heat transfer from an isothermal and isoflux sphere in the steady symmetric flow regime. Int. J. heat and mass transfer. 49, 984-994.
9. Dixon A. G., Taskin M. E., Nijemesisland M., Stitt E. H., 2011. Systematic mesh development for 3D CFD simulation of fixed beds: Single sphere study. Comp. Chem. Eng., 35, 1171-1185.
10. Fornberg B., 1988. Steady viscous flow past a sphere at high Reynolds numbers. J. Fluid Mech.190, 471-489.
11. Feng Z., Michaelides E. E., 2000. A numerical study on transient heat transfer from a sphere at high Reynolds and Peclet numbers. Int. J. Heat and Mass transfer. 43, 219-229.
12. Gushchin V. A., Matyushin R. V., 2006. Vortex formation mechanisms in the wake behind a sphere for $200 \leq Re \leq 380$. Fluid Dyn. 41,N°5,795-809.
13. Johnson T. A., Patel V. C. (1999). Flow past a sphere up to a Reynolds number of 300. J. Fluid Mech. 378, 19-70.
14. Kechroud N., Brahimi M., Djati A. (2010a). Characterization of dynamic behavior of the continuous phase in liquid fluidized bed. Powder Tech., 200, issue 3, 149-157.
15. Kechroud N., Brahimi M., Djati A. (2010b). Spectral analysis of dynamic behavior of the continuous phase in liquid fluidized bed. " Proc. of 7th Int. Conf. on Multiphase Flow .," Tampa Fl, USA, May 30 –June 4, pp.1-7
16. Lee S., (2000). A numerical study of the unsteady wake behind a sphere in a uniform flow at moderate Reynolds numbers. Comp. Fluids, 29,639-667.
17. Lin C. L., Lee S. C., (1973). Transient state analysis of separated flow around a sphere. Comp. Fluids, 1,235-250.
18. Magnaudet J., Rivero M.,Fabre J., (1995). Flows past a rigid sphere or a spherical bubble.1. steady straining flow. J. Fluid Mech., 284, 97-135.
19. Masliyah J. H., (1972). Steady wakes behind oblate spheroids: flow visualization. Physics of fluids 16, 6-8.
20. Nakamura, I., (1976). Steady wake behind a sphere. Physics of fluids. 19, 5-8.
21. Reddy R. K., Joshi J. B., Nandakumar K., Minev P. D., (2010). Direct numerical simulations of a freely falling sphere using fictitious domain method: Breaking of axisymmetric wake. Chem. Eng. Sc.,65, 2159-2171
22. Richter A., Nikrityuk P. A., (2012). Drag forces and heat transfer coefficients for spherical, cuboidal and ellipsoidal particles in cross flow at sub-critical Reynolds numbers.Int. J. heat and mass transfer,55, 1343-1354
23. Rimon Y., Cheng J., (1969). Numerical solution of a uniform flow over a sphere at intermediate Reynolds numbers. Phys. Fluids 12, N°5, 949-959
24. Sekhar T. V. S., Hema Sundar Raju B., (2012). Higher-Order compact scheme for the incompressible Navier-Stokes equations in spherical geometry,Commun. Comput. Phys., 11, N°1, 99—113.
25. Smith P. A., Stansby P. K., (1988). Impulsively started flow around a circular cylinder by the vortex method. J. Fluid Mech., 194, 45-77.
26. Taneda S.,(1956). Experimental investigation of the wake behind a sphere at low Reynolds numbers. Journal of the physical society of Japan, 11, 1104-1108.
27. Ta Phuoc Loc, Bouard R., (1985). Numerical solution of the early stage of the unsteady viscous flow around a circular cylinder: a comparison with experimental visualization and measurements. J. Fluid Mech., 160, 93-117.

28. Ta Phuoc Loc, (1980). Numerical analysis of unsteady secondary vortices generated by an impulsively started circular cylinder. J. Fluid Mech., 100,111-128.

28. Thoman D. C., Szewczyk A. A., (1969). Time-dependant viscous flow over a circular cylinder. Phys. Fluids Suppl., 12, 76-87.
29. Turton R., Levenspiel O., (1986). A short note on the drag correlation for spheres. Powd. Tech.47, 83-86.